24th Australasian Fluid Mechanics Conference – AFMC2024
Canberra Australia
1-5 December 2024

Paper No: AFMC2024-353
DOI:10.5281/zenodo.14213632

Parametric Study of PEM Water Electrolyzer for Green Hydrogen Production

Ali Bayat [1], Prodip K. Das [2], Goutam Saha [1] and Suvash C. Saha [1*]

[1] School of Mechanical and Mechatronics Engineering, University of Technology Sydney, NSW, Australia
[2] School of Engineering, The University of Edinburgh, Edinburgh, United Kingdom
* Email: Suvash.Saha@uts.edu.au

Abstract

Hydrogen is emerging as a pivotal component of sustainable and eco-friendly energy systems, garnering increasing global attention, particularly within the industrial and transportation sectors. As nations strive towards net-zero emissions, green hydrogen production becomes paramount. Among hydrogen production methods, proton exchange membrane (PEM) water electrolysis stands out for generating green hydrogen by utilizing renewable energy sources to split water molecules into hydrogen and oxygen. It offers high-purity hydrogen, operates efficiently across a wide range of current densities, responds swiftly to changes, and is well-suited for integration with intermittent renewable energy sources like wind and solar. Various attempts have been made to simulate the PEM system, from models focusing on electrochemical reactions to those including fluid mechanics. This study focuses on single-phase flow combined with detailed chemical reactions for a typical single-cell PEM electrolyzer. A 3D numerical approach using COMSOL Multiphysics is utilized for a parametric study on system performance. The impact of configurational features of the membrane on hydrogen production is studied, with emphasis on the polarization curve as the main indicator, the electrolyte and electrode potentials, and hydrogen mole distribution. Our findings provide insights to enhance design and operational strategies, making hydrogen a viable and sustainable energy carrier for the future.

1. Introduction

Hydrogen has garnered significant attention as a clean and versatile energy carrier, capable of contributing to heat and power supply across various sectors (Qazi, 2022). Recently, there has been significant growth in the number of projects aimed at producing net-zero emission hydrogen, also known as green hydrogen (Incer-Valverde *et al.*, 2023). In the early 2000s, hydrogen accounted for only 7% of all energy sources; today, that figure has surged to 22%. Substantial investments have been made to further increase this share, with a target of reaching 50% by 2030 (Ajanovic *et al.*, 2022). One notable example of this effort is Australia. Australia's transition to a greener future hinge on replacing fossil fuels with hydrogen, not only in automobiles (via fuel cells) but also in industrial and residential sectors, replacing natural gas. Moreover, the ease of storing and transporting hydrogen in the form of ammonia (NH_3) positions it as a promising source for fertilizing lands, known as green ammonia (Negro *et al.*, 2023) .

Hydrogen is mainly found in nature in compound molecules, the most important of which is water. Electrolysing water using electricity to split it into hydrogen and oxygen offers a contamination-free hydrogen source which can be used in fuel cells, energy storage, metal refining, chemical production, and hydrogen fueling stations (Das *et al.*, 2023). Among the most common industrial methods of water electrolysis, the proton exchange membrane (PEM) water electrolyzer has drawn significant attention due to its high-purity hydrogen production even at low temperatures, its fast response to input parameters, and its compact design (Ma *et al.*, 2021; Zheng *et al.*, 2023).

Various attempts have been made to simulate the PEM water electrolyzer system. Some studies, such simply analysed the electrochemical reactions in a PEM cell without considering the fluid flow

in the components (Choi *et al.*, 2004). Later, the effect of water flow in the anode, alongside the formation of oxygen and hydrogen in the anode and cathode, was investigated using single-phase flow. In most previous works, the flow was considered only in the form of gas, meaning the interaction between gas and liquid was not accounted for (Nie *et al.*, 2009; Toghyani *et al.*, 2018; Ubong *et al.*, 2009). Although the complexity and accuracy of single-phase flow analysis are not as high as those of two-phase flows (Corda *et al.*, 2023; Jiang *et al.*, 2023; Ma *et al.*, 2021; Zheng *et al.*, 2023), single-phase flow still offers a valuable method for PEM electrolysis analysis. It allows for a fast-numerical process with good control over optimization and control processes in PEM systems.

This study focuses on single-phase flow combined with detailed chemical reactions for a typical single-cell PEM. The electrical and configurational effects of the membrane, as the most crucial component of the PEM, on hydrogen production and cell performance have been investigated in a parametric study. The results are presented in the form of a polarization plot, which serves as the main indicator of PEM performance, as well as the molar distribution of hydrogen and the electrode and electrolyte potential in a typical PEM electrolysis cell. Although sensitivity analysis offers the optimal values for the PEM to achieve maximum efficiency, heat transfer and stability considerations are also discussed to explain the limitations in real-life setups.

2. Physical Domain and Mathematical Modelling

2.1 Geometrical Domain

The physical domain (Figure 1) used for this study consists of a membrane layer coated with two catalyst layers (CLs) on both sides, each with a thickness of 20 μm. The membrane is made of Nafion 117 with a thickness of 183 μm. Immediately after the CLs, there is a porous transport layer (PTL) that facilitates the process of ion transfer. Two bipolar plates (BPs) with a length of 5 cm (cell length) and a width of 1.5 mm at the inlets and outlets are considered (Jiang *et al.*, 2023).

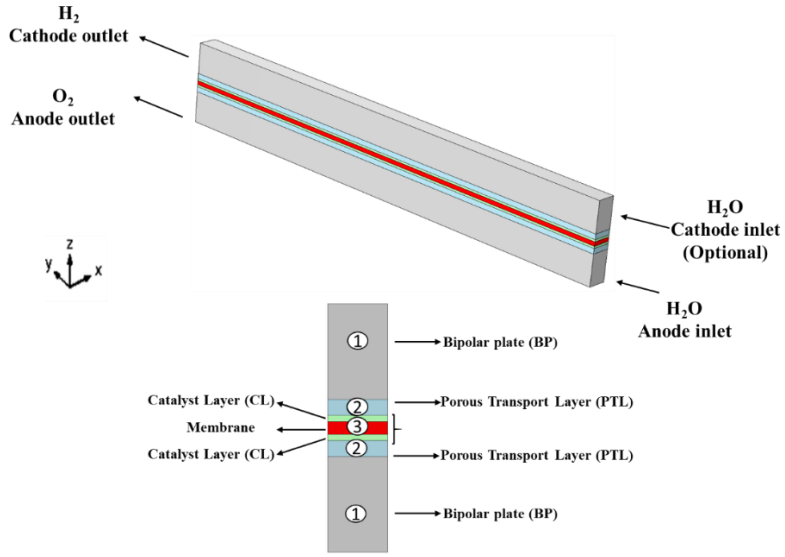

Figure 1. Top: Schematic of a PEM water electrolyzer. Bottom: 2-D cross-section

2.2 Modelling Assumptions

The water flow at the anode inlet is considered fully developed. An optional water flow is introduced at the cathode inlet to facilitate computational simulation (in real-world setups, this prevents membrane dryness). The membrane is assumed to be ideal, meaning there is no crossover for species such as hydrogen and oxygen; only protons (H^+) are allowed to pass through. CLs and PTLs are assumed to be homogeneous, isotropic porous media. The flow is treated as incompressible and laminar, and the produced gases are assumed to behave as ideal gases. To ensure numerical accuracy, a mesh independence test and sensitivity analysis were conducted. The modeling assumptions, such as single-phase flow and isotropic properties, align with established literature and provide a balance between computational efficiency and result reliability, accurately capturing the essential PEMEC behaviour.

2.3 Electrochemical Reactions

Water flow at the anode inlet within the bipolar plates passes through the PTL and CL, where it splits into oxygen (O_2), protons (H^+), and electrons (e^-) utilizing electricity. The protons (H^+) pass through the membrane and reach the cathode CL, where they combine with electrons that have travelled through an external circuit to form hydrogen (H_2) (Ma *et al.*, 2021). Hydrogen (H_2) and oxygen (O_2) are then collected at the cathode and anode outlets, respectively (eq. (1) and eq. (2)).

$$H_2O \rightarrow 0.5O_2 + 2H^+ + 2e^- \quad \text{(Anode)} \tag{1}$$

$$2H^+ + 2e^- \rightarrow H_2 \quad \text{(Cathode)} \tag{2}$$

The governing equations for proton and electron transport are presented in eq. (3) and eq. (4).

$$\nabla.\left(\sigma_m^{eff}\,\nabla\varphi_m\right) + B_{\varphi_m} = 0 \tag{3}$$

$$\nabla.\left(\sigma_e^{eff}\,\nabla\varphi_e\right) + B_{\varphi_e} = 0 \tag{4}$$

where φ_m and φ_e represent the membrane and electrode potentials, σ_m^{eff} and σ_e^{eff} represent the effective conductivities of membrane and electrode, and B_{φ_m} and B_{φ_e} are the source terms, both of which equate to the current density (i). The effective conductivity of membrane is defined by Bruggeman correlation as eq. (5) (Bruggeman, 1935; Das *et al.*, 2010).

$$\sigma_m^{eff} = 100\,{\varepsilon_m}^{1.5}(0.005139\lambda - 0.00326)exp[1268\left(\frac{1}{303} - \frac{1}{T}\right)] \tag{5}$$

where λ represents the membrane's water content, which ranges between 14 and 22, T is the absolute temperature, and ε_m represent the ratio of the membrane volume to the total cell volume. To calculate the σ_e^{eff}, the Bruggeman correlation is also considered, as presented in eq. (6).

$$\sigma_e^{eff} = \sigma_e\,(1-\varepsilon)^{1.5} \tag{6}$$

where σ_e and ε represent the intrinsic conductivity and the porosity of the electrodes, respectively (Bruggeman, 1935; Reshetenko *et al.*, 2020).

2.4 Fluid Flow

The continuity equation in the form of steady states (eq. (7)) is utilized for the single-phase flow within the PEM components, including porous components such as CLs and PTLs, as well as non-porous components such as BPs and the membrane (Jiang *et al.*, 2023).

$$\nabla.(\rho\varepsilon\boldsymbol{u}) = B_j \tag{7}$$

where ρ and u represent the density and velocity vector, respectively. B_j is the source term for reactive species in the electrolysis process, which can be formulated using Faraday's law. (eq. (8)).

$$\begin{cases} B_{H_2O} = -\frac{i_a M_{H_2O}}{2F} \\ B_{H_2} = \frac{i_c M_{H_2}}{2F} \\ B_{O_2} = \frac{i_a M_{O_2}}{4F} \end{cases} \tag{8}$$

where M denotes the molecular weight of the species, F is the Faraday's constant, and i_c and i_a represent the current density at the cathode and anode, respectively (Ramousse *et al.*, 2008).

Assuming a Newtonian fluid, a steady-state momentum equation for a single-phase flow can be formulated as shown in eq. (9) (Jiang *et al.*, 2023).

$$\nabla.(\rho\varepsilon\boldsymbol{u}\boldsymbol{u}) = -\varepsilon\,\nabla p + \nabla.[\,\mu\,(\nabla\boldsymbol{u} + (\nabla\boldsymbol{u})^T)] - \frac{\mu}{\kappa}\varepsilon^2\boldsymbol{u} \tag{9}$$

where μ and p represent the dynamic viscosity and pressure, respectively. κ is the permeability of the porous media, which can be determined using Kozeny-Carman correlation relating it to the porosity and the particle size (D_P), as presented in eq. (10) (Carman, 1956).

$$\kappa = \frac{D_P^2}{180}\frac{\varepsilon^3}{(1-\varepsilon)^2} \tag{10}$$

2.5 Boundary Conditions

A velocity of 0.1 m/s is considered at the anode inlet for water, corresponding to a molar fraction of 1. Electrically, the cathode cell is considered to have a potential of zero, while the anode side has a potential of 1.229 V (Jiang *et al.*, 2023). The reference pressure is set to 1 atm. The electrode conductivity of the CLs and PTLs is considered constant within the temperature range of this study. A no-slip condition is assumed at the walls for the momentum equation.

3. Methodology

3.1 Computational Modeling

A 3D numerical simulation was performed in COMSOL Multiphysics 6.1 using modules for free and porous media flows for the components, interconnected by a water electrolyzer module. The 3D geometry of a standard PEM electrolyzer was constructed, following specific geometric features. A table of physical parameters supported the parametric study, with fluid properties computed using the coupled reacting flow interface for H_2 and O_2. A tailored mesh utilized symmetry. A five-stage solver strategy ensured precise results: initial stationary solver for primary current distribution, secondary solver for overpotentials, and subsequent solvers for anode and cathode flows, culminating in a final simultaneous solution. An auxiliary sweep parameter aided convergence.

3.2 Sensitivity Analysis

To determine the importance of various input parameters on the efficiency of a PEM water electrolyzer, a local sensitivity analysis was conducted (Saltelli *et al.*, 2008). Configurational features i.e. membrane thickness and membrane electrical conductivity was considered for this analysis. These two parameters were investigated within their respective ranges, considering a 10 percent change in their values. The normalized sensitivity indices were then calculated by approximating the partial derivatives with the average gradient at the nominal operating point (NOP). The sensitivity index of an output parameter like H with respect to input factor w can be calculated using eq. (11) as follows (Gustafson *et al.*, 1996):

$$S_w^Z = \frac{\partial Z}{\partial w}\Big|_{NOP} . \frac{w_0}{Z_0} \tag{11}$$

where $\frac{\partial H}{\partial w}\Big|_{NOP}$ denotes the partial derivative of Z with respect to w , evaluated at a nominal operating point (NOP). w_0 and Z_0 are the nominal value of w and Z.

4. Results and Discussion

In this section, the results obtained from numerical simulations are presented. Section 4.1 discusses the effect of membrane thinning on the polarization plot, electrode and electrolyte potential, and hydrogen distribution across the entire PEM cell, particularly at the cathode outlet. Section 4.2 examines the impact of boosting the membrane's electrical conductivity (within the real industrial range with actual values), focusing on the same diagrams mentioned in Section 4.1. Section 4.3 presents a local sensitivity analysis chart highlighting the most important parameters and their impact on PEM performance, with an emphasis on the average current density of the cell as the output parameter.

4.1 Impact of Membrane Thickness

The membrane plays a key role in the process of hydrogen production in a PEM water electrolyzer cell. A thinner membrane allows more passage of H^+ ions, consequently increasing hydrogen production. In an ideal membrane—without crossover phenomena for other species like H_2 and O_2—decreasing the membrane thickness results in a lower required voltage to achieve the specified current density. In other words, at the same given voltage, a PEM cell with a thinner membrane (assuming all other properties are the same) will produce a higher current density. However, the main issue with thinner membranes is heat transfer and thermal management, which can adversely affect PEM stability in the long run. This can lead to increased crossover, particularly of hydrogen, and pose safety issues. Figure 2a demonstrates the potential distribution over the membrane electrode assembly

(MEA) for two different membrane thicknesses. It shows that the thinner membrane (100 µm) exhibits a steeper potential drop from anode to cathode, indicating a faster rate of potential change (see also Figure .1). Figure 2b presents the polarization plot for the two different membrane thicknesses, showing that a higher voltage is required to produce the same current density for the thicker membrane. Figure 2c illustrates the hydrogen mole distribution across the entire cathode compartment, indicating that the rate of hydrogen production for the thinner membrane (100 µm) is higher compared to the thicker membrane, resulting in a more efficient system.

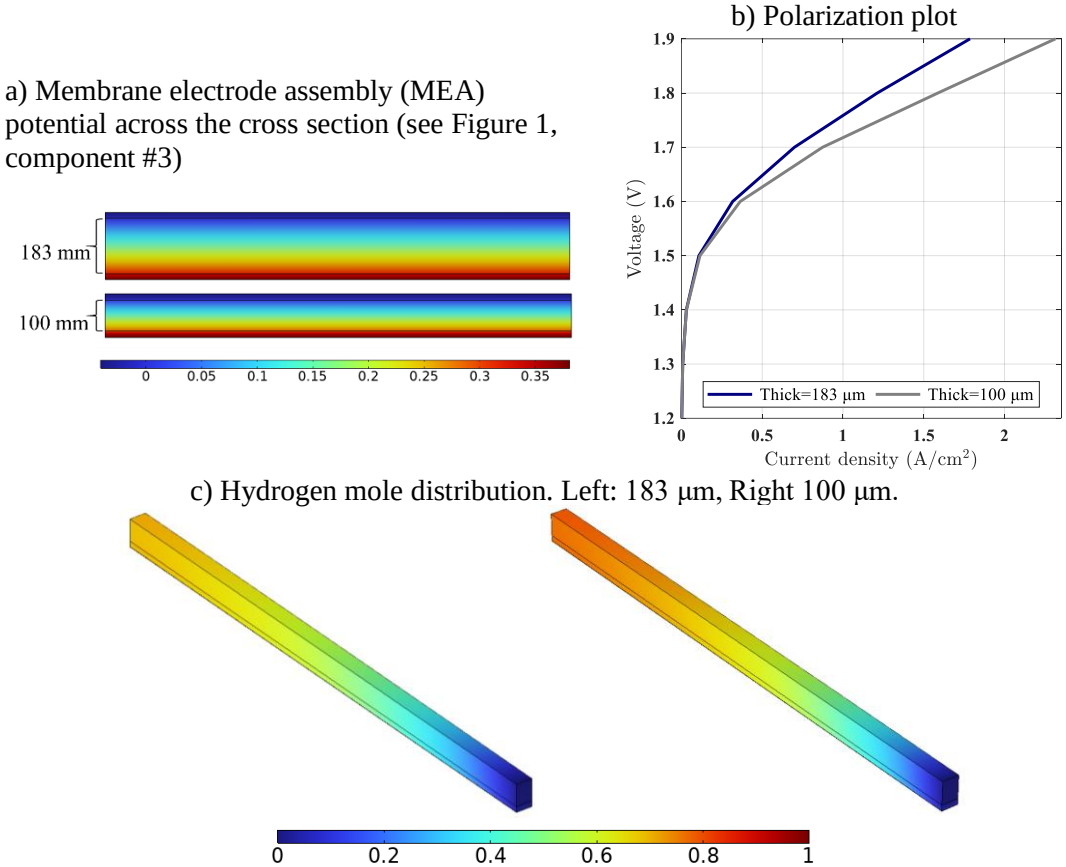

Figure 2. Numerical results analysing the effect of membrane thickness on PEM cell performance

4.2 Impact of Membrane Electrical Conductivity

The electrical conductivity of a membrane is an intrinsic property that reflects its potential for passing electric current. Eq. (5) shows that the effective membrane conductivity is not only a function of the water content (λ) and the temperature (T), but also depends on the ratio of the membrane volume to the total cell volume. Additionally, the porosity of the catalyst layers (CLs) and porous transport layers (PTLs) can directly impact the membrane volume fraction and, consequently, the effective membrane conductivity. Overall, higher intrinsic conductivity and the optimal configuration of the membrane electrode assembly (MEA) can enhance the effective conductivity, leading to increased hydrogen production through improved ion transport. Figure 3a presents the polarization plot for two different membrane conductivities, showing that at a given voltage, the current density produced by the higher conductivity membrane is greater than that of the lower conductivity membrane. The result is compared with experimental data for a membrane thickness of 183 µm. Figure 3b illustrates the hydrogen mole distribution across the entire cathode compartment, indicating that the rate of hydrogen production for the membrane with higher conductivity is greater compared to the lower conductivity membrane, resulting in a more efficient system. The maximum hydrogen mole concentrations for σ_m = 7 S/m and σ_m= 10 S/m are 0.767 and 0.813, respectively.

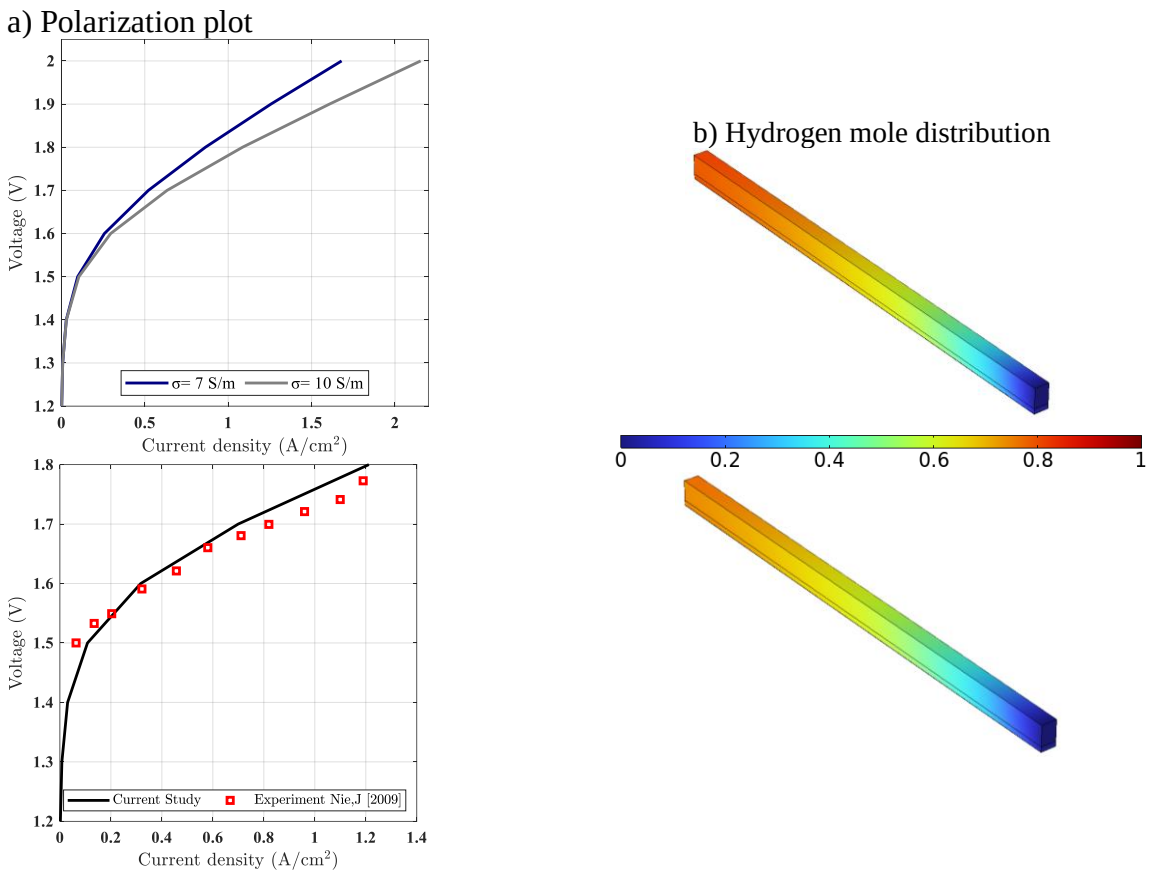

Figure 3. Numerical results analysing the effect of membrane conductivity on PEM cell performance

4.3 Local Sensitivity Analysis

Considering two main configurational features of a PEM cell, namely membrane thickness and conductivity, and conducting the local sensitivity analysis as presented in Figure 4, it is evident that membrane conductivity has the highest and most direct positive effect on cell performance, with an index of 0.68 showing that boosting conductivity greatly enhance ion transport and overall cell efficiency. In contrast, membrane thickness has a negative effect, with a value of -0.54 showing that an increase in membrane thickness significantly reduces current density.

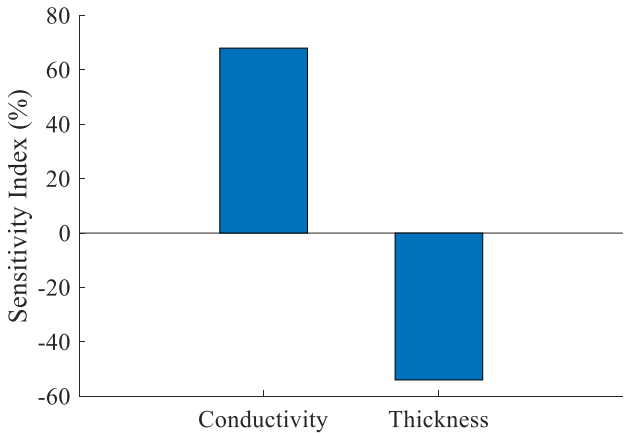

Figure 4. Sensitivity indices for a 10% change in the nominal values

While thinner membranes with higher conductivity indeed enhance the performance of PEM cells by reducing resistance and improving efficiency, ignoring heat transfer considerations and membrane stability can lead to significant issues. Thinner membranes are more susceptible to thermal degradation and mechanical failure due to their reduced structural integrity. Inadequate heat management can cause localized overheating, leading to hotspots that accelerate membrane degradation and reduce its lifespan. Additionally, higher conductivity membranes may be prone to

chemical degradation in the harsh operational environment of a PEM cell, resulting in a loss of conductivity over time. Ensuring efficient heat dissipation and addressing the mechanical and chemical stability of the membrane are crucial to maintaining long-term performance and reliability in real-life industrial applications.

5. Conclusions

This study provides a parametric analysis of a single-cell PEM water electrolyzer, focusing on the impacts of membrane thickness and electrical conductivity on cell performance. Through detailed numerical simulations, it has been demonstrated that while thinner membranes and higher electrical conductivity significantly enhance hydrogen production by improving ion transport and reducing resistance, these optimal conditions pose challenges in real-life applications. Issues related to heat transfer, thermal management, and membrane stability highlight the importance of balancing performance improvements with practical considerations. The findings underscore the need for careful design and material selection to ensure both high efficiency and long-term durability in industrial PEM electrolyzer systems for green hydrogen production.

Acknowledgments

The authors acknowledge the computation resources provided by the high-performance computing facility of the University of Technology Sydney (UTS). The first author acknowledges the receipt of UTS PhD scholarship for the pursuit of this study.

Nomenclature

B_j	Source term in mass conservation equation [kg/ (m^3 s)]
BP	Bipolar plates
CL	Catalyst layer
D_P	Particle diameter of porous material [m]
F	Faraday's constant, 896485.3 [C/mol]
H^+	Proton
i	Current density [A/m^2]
M	Molecular weight of species [kg/mol]
MEA	Membrane Electrode Assembly
p	Pressure [Pa]
PEM	Proton Exchange membrane
PTL	Porous Transport Layer
T	Temperature [°C or K]
$\boldsymbol{u}$	Velocity vector [m/s]
w	Input factor in sensitivity analysis
Z	Output factor in sensitivity analysis

Greek Symbols

ε	Porosity
κ	Permeability of porous medium [m2]
λ	Membrane's water content [g H_2O/g dry membrane]
μ	Dynamic viscosity [Pa. s]
ρ	Density [kg/m^3]
σ	Electrical conductivity [S/m]
φ	potential

Subscript and superscript

a	Anode
c	Cathode
e	Electrode
eff	Effective
m	Membrane

References

Ajanovic, A., Sayer, M.& Haas, R. 2022, The economics and the environmental benignity of different colors of hydrogen, *International journal of hydrogen energy*, **47**(57), 24136-24154.

Bruggeman, V. D. 1935, Berechnung verschiedener physikalischer Konstanten von heterogenen Substanzen. I. Dielektrizitätskonstanten und Leitfähigkeiten der Mischkörper aus isotropen Substanzen, *Annalen der physik*, **416**(7), 636-664.

Carman, P. C. 1956, Flow of gases through porous media, *(No Title)*.

Choi, P., Bessarabov, D. G.& Datta, R. 2004, A simple model for solid polymer electrolyte (SPE) water electrolysis, *Solid State Ionics*, **175**(1-4), 535-539.

Corda, G., Cucurachi, A., Fontanesi, S.& d'Adamo, A. 2023, Three-Dimensional CFD Simulation of a Proton Exchange Membrane Electrolysis Cell, *Energies*, **16**(16), 5968.

Das, P. K., Jiao, K., Wang, Y., Barbir, F.& Li, X. 2023, *Fuel Cells for Transportation: Fundamental Principles and Applications*, Elsevier.

Das, P. K., Li, X.& Liu, Z.-S. 2010, Effective transport coefficients in PEM fuel cell catalyst and gas diffusion layers: Beyond Bruggeman approximation, *Applied Energy*, **87**(9), 2785-2796.

Gustafson, P., Srinivasan, C.& Wasserman, L. 1996, Local sensitivity analysis, *Bayesian statistics*, **5**, 197-210.

Incer-Valverde, J., Korayem, A., Tsatsaronis, G.& Morosuk, T. 2023, "Colors" of hydrogen: Definitions and carbon intensity, *Energy Conversion and Management*, **291**, 117294.

Jiang, Y., Li, Y., Ding, Y., Hu, S., Dang, J., Yang, F.& Ouyang, M. 2023, Simulation and experiment study on two-phase flow characteristics of proton exchange membrane electrolysis cell, *Journal of power sources*, **553**, 232303.

Ma, Z., Witteman, L., Wrubel, J. A.& Bender, G. 2021, A comprehensive modeling method for proton exchange membrane electrolyzer development, *International journal of hydrogen energy*, **46**(34), 17627-17643.

Negro, V., Noussan, M.& Chiaramonti, D. 2023, The potential role of ammonia for hydrogen storage and transport: A critical review of challenges and opportunities, *Energies*, **16**(17), 6192.

Nie, J., Chen, Y., Cohen, S., Carter, B. D.& Boehm, R. F. 2009, Numerical and experimental study of three-dimensional fluid flow in the bipolar plate of a PEM electrolysis cell, *International journal of thermal sciences*, **48**(10), 1914-1922.

Qazi, U. Y. 2022, Future of hydrogen as an alternative fuel for next-generation industrial applications; challenges and expected opportunities, *Energies*, **15**(13), 4741.

Ramousse, J., Didierjean, S., Lottin, O.& Maillet, D. 2008, Estimation of the effective thermal conductivity of carbon felts used as PEMFC Gas Diffusion Layers, *International journal of thermal sciences*, **47**(1), 1-6.

Reshetenko, T., Serov, A., Odgaard, M., Randolf, G., Osmieri, L.& Kulikovsky, A. 2020, Electron and proton conductivity of Fe-NC cathodes for PEM fuel cells: A model-based electrochemical impedance spectroscopy measurement, *Electrochemistry communications*, **118**, 106795.

Saltelli, A., Ratto, M., Andres, T., Campolongo, F., Cariboni, J., Gatelli, D., Saisana, M.& Tarantola, S. 2008, *Global sensitivity analysis: the primer*, John Wiley & Sons.

Toghyani, S., Afshari, E.& Baniasadi, E. 2018, Metal foams as flow distributors in comparison with serpentine and parallel flow fields in proton exchange membrane electrolyzer cells, *Electrochimica acta*, **290**, 506-519.

Ubong, E., Shi, Z.& Wang, X. 2009, Three-dimensional modeling and experimental study of a high temperature PBI-based PEM fuel cell, *Journal of the Electrochemical Society*, **156**(10), B1276.

Zheng, J., Kang, Z., Han, B.& Mo, J. 2023, Three-Dimensional Numerical Simulation of the Performance and Transport Phenomena of Oxygen Evolution Reactions in a Proton Exchange Membrane Water Electrolyzer, *Materials*, **16**(3), 1310.